A Robust Dynamic Screening System By Estimation of the Longitudinal Data Distribution

Lu You and Peihua Qiu
Department of Biostatistics
University of Florida
Gainesville, FL 32610

Abstract

To online monitor the longitudinal performance of processes and give early signals to processes with irregular patterns, a series of dynamic screening systems (DySS) have been proposed in the literature. Existing DySS methods are all based on estimation of the in-control (IC) mean and variance of processes with a regular longitudinal pattern. In this paper, a new DySS method is suggested, which is based on estimation of the IC distribution of processes with a regular longitudinal pattern. Based on the estimated IC distribution, a statistical process control chart is constructed for sequentially detecting any distributional shifts in a longitudinal process. The suggested control chart is relatively simple to design and implement, and it is robust to the true IC distribution. Numerical examples show that it outperforms some representative existing DySS methods. These properties make it an ideal tool for dynamic screening applications, which is demonstrated by a real-data example.

Key Words: Data correlation; Dynamic processes; Longitudinal pattern; Normalization; Online monitoring; Transformation.

1 Introduction

In practice, dynamic processes whose in-control (IC) distribution changes over time are common. For instance, durable goods (e.g., airplanes, computers) often need to be checked regularly or occasionally for certain performance variables. The distribution of such performance variables would change when the durable goods get older, even when they perform normally at their ages. The research problem to monitor the longitudinal performance of such a dynamic process is called dynamic screening (DS) in the literature (cf., Qiu and Xiang 2014). This paper aims to develop a new method for handling DS applications effectively.

Statistical process control (SPC) charts provide a popular tool for online process monitoring (Hawkins and Olwell 1998, Montgomery 2012, Qiu 2014). However, SPC methods are mainly for monitoring production lines in manufacturing industries, and most of them are designed based on the assumptions that process observations are independent and identically distributed at different observation times. These assumptions are obviously invalid in many DS applications because the IC process distribution can change over time in these applications. For this reason, Qiu and Xiang (2014) proposed the first dynamic screening system (DySS) to handle univariate DS problems. This method consists of three main steps. First, the regular longitudinal pattern of the dynamic process under monitoring is first estimated from an IC data that contain the observed data of some IC dynamic processes. Second, the observed data of the dynamic process under monitoring is standardized by using the estimated regular longitudinal pattern. Third, a control chart is applied to the standardized observations to check whether the longitudinal pattern of the process under monitoring is significantly different from the estimated regular longitudinal pattern and a signal is given once a significant difference is detected. In the real data example about the Framingham heart study that will be discussed in more details in Section 4, we would like to detect the occurrence of strokes early by sequentially monitoring patients' systolic blood pressure readings. By using the DySS method, the regular longitudinal pattern of the systolic blood pressure needs to be first estimated from a dataset of some non-stroke patients. Then, for a new patient to monitor, we can standardize his/her observations using the estimated longitudinal pattern and then monitor the standardized observations by a control chart. This univariate method was generalized to multivariate cases in Qiu and Xiang (2015). Cases with serially correlated data were discussed in Li and Qiu (2016, 2017). Certain modifications and improvements of these charts were discussed in Li et al. (2018), Qiu et al. (2018), and Qiu et al. (2020).

It should be pointed out that the DS problem discussed in this paper is completely different from the profile monitoring problem discussed extensively in the SPC literature (e.g., Kang and Albin 2000, Qiu et al. 2010). In the profile monitoring problem, we are mainly concerned about the functional relationship between a response variable and some covariates, and the collected data of a process at each time point are a set of observations of the response variable and the covariates(i.e., profiles). Then, a profile monitoring method is for sequentially monitoring the sequence of profiles collected at different time points. As a comparison, our ultimate goal in the current DS problem is to sequentially monitor the longitudinal pattern of each individual subject and the observed data

of an individual subject at each time point is usually a single value of the performance variables. Thus, the DS problem is the same as the conventional process monitoring problem, except that the IC process distribution could change over time in the DS problem while it is often assumed unchanged over time in the conventional process monitoring problem. Although observations of each individual subject look like a profile in the DS problem, each individual is actually treated as a separate process and we are interested in monitoring the longitudinal behavior of each individual in that problem.

In all the DySS methods mentioned above, the regular longitudinal pattern of a dynamic process is described by its mean and covariance functions. This may not be appropriate in cases when the time-varying process distribution is non-Gaussian. In practice, the true distribution of a dynamic process is rarely Gaussian. So, a natural idea to improve the existing DySS methods is to describe the regular longitudinal pattern of a dynamic process by the entire IC process distribution which could change over time. Then, a control chart can be applied to the observations of the dynamic process that are standardized by using the estimated IC process distribution. Based on this idea, we develop a new and effective DySS method in this paper. Compared to the existing DySS methods, the proposed new method has two major advantages. First, its design is relatively simple because the control limit of its control chart can be determined conveniently by a Monte Carlo simulation, as discussed in detail in Section 2. As a comparison, the control limits of the control charts involved in most existing DySS methods need to be computed by some relatively complicated resampling procedures from an IC dataset. Second, the proposed new method is robust to the true IC process distribution without sacrificing information in the observed data. As a comparison, the existing DySS methods are either sensitive to the true IC process distribution (e.g., Qiu and Xiang 2014) or losing some effectiveness due to the fact that they need to use nonparametric control charts that are based on the categorized data or the ordering information of the original process observations (e.g., Li and Qiu 2016). Numerical examples in Section 3 will show that the proposed method indeed outperforms some representative existing DySS methods in various different cases considered.

The remainder of the paper is organized as follows. In Section 2, the proposed new DySS method will be described in detail. Some simulation studies are presented in Section 3 to evaluate its numerical performance. In Section 4, the proposed method is applied to a real-data example about the well-known Framingham heart study. Finally, Section 5 concludes the paper with some comments and remarks.

2 Proposed New Method

As mentioned in Section 1, the novelty of the proposed method is mainly in describing the regular longitudinal pattern of an IC dynamic process by the entire IC process distribution. Estimation of this time-varying distribution and construction of the subsequent online monitoring scheme are discussed in the two parts below.

2.1 Modeling the Regular Longitudinal Pattern of an IC Dynamic Process

Assume that we want to describe and estimate the regular longitudinal pattern of the performance variable $y(t)$ and there are observed data of n IC dynamic processes of $y(t)$. Observations of the ith IC dynamic process $y_i(t)$ are obtained at the times $\{t_{i1}, t_{i2}, \ldots, t_{im_i}\}$, where the observation times could be unequally spaced in the time interval $[0, T]$ and $y_i(t)$ are assumed to be independent realizations of $y(t)$, for $i = 1, 2, \ldots, n$. Let $F(q;t) = \mathrm{P}(y(t) \le q)$ be the cumulative distribution function (cdf) of $y(t)$. In this paper, we assume that $F(q;t)$ is a continuous function of both t and q. This assumption implies that the performance variable $y(t)$ has a continuous IC cdf at any given t and the cdf changes continuously over t, which should be reasonable in many applications including the one about the Framingham heart study discussed in Section 1. Then, $F(q;t)$ can be used for describing the regular longitudinal pattern of $y(t)$. In the example of the Framingham heart study, the performance variable of interest is the systolic blood pressure, $F(q;t)$ is its IC cdf at time t, and $F(q;t)$ can be estimated from an IC data to describe the regular longitudinal pattern of the systolic blood pressure.

To estimate $F(q;t)$ from the observed data $\{y_i(t_{ij}), j = 1, 2, \ldots, m_i, i = 1, 2, \ldots, n\}$ of the n IC dynamic processes, one natural idea is to use the local kernel smoothing method that was discussed in Fan et al. (1996) and Yu and Jones (1998). To this end, let $W(\cdot)$ be a pre-specified cdf kernel function, and $W_{h_w}(\cdot) = W(\cdot/h_w)$, where $h_w > 0$ is a bandwidth parameter. Then, for any value of q, $F(q;t)$ can estimated by

$$\widehat{F}(q;t) = \arg\min_{a \ge 0} \sum_{i=1}^{n} \sum_{j=1}^{m_i} \left[W_{h_w}(q - y_i(t_{ij})) - a\right]^2 K_{h_f}(t_{ij} - t), \tag{1}$$

where $h_f > 0$ is another bandwidth parameter, and $K_{h_f}(\cdot) = K(\cdot/h_f)/h_f$ is a symmetric density kernel function. In (1), two kernel functions $W(\cdot)$ and $K(\cdot)$ are used. Thus, this estimation procedure is often called a double-kernel smoother in the literature (cf., Yu and Jones 1998). In this

paper, the density kernel function $K(\cdot)$ is chosen to be the Epanechnikov kernel function, namely, $K(s) = 0.75(1-s^2)I(|s| \le 1)$, because of its good statistical properties (cf., Epanechnikov 1969). To ensure that the estimate $\widehat{F}(q;t)$ takes values in the entire interval $(0,1)$, the cdf kernel function $W(\cdot)$ should not have a compact support. To meet this requirement, we adopt the suggestion in Yu and Jones (1998) to choose $W(\cdot)$ to be the standard normal cdf in this paper. Namely, we choose $W(t) = \frac{1}{\sqrt{2\pi}} \int_{-\infty}^{t} \exp(-s^2/2)\, ds$.

In the above estimation procedure, there are two bandwidth parameters h_w and h_f that need to be specified in advance. To this end, by the normal referencing rule proposed by Silverman (1986) and Fan and Gijbels (1995), h_w can be chosen to be

$$h_w = \frac{\int_0^T \widehat{\sigma}(t)\, dt}{T} \left[\frac{8\pi^{1/2} \int w^2(t)\, dt}{3\{\int t^2 w(t)\, dt\}^2 \sum_{i=1}^n m_i} \right]^{1/5},$$

where $\widehat{\sigma}^2(t)$ is an estimate of $\sigma^2(t) = \sigma^2_{y(t)}$, and $w(t) = dW(t)/dt$ is the density function of $W(t)$. Here, $\widehat{\sigma}^2(t)$ can be obtained using the kernel smoothing estimation discussed in Qiu and Xiang (2014). To choose the bandwidth parameter h_f, we can consider using the following residual squares criterion, which is similar to the one discussed in Fan et al. (1996):

$$\mathrm{RSC}(h_f) = \sum_{i=1}^{n} \sum_{j=1}^{m_i} \tau^2(y_i(t_{ij}), t_{ij}; h_f) \left[1 + 3S_0(t_{ij})/V_0(t_{ij})^2\right],$$

where

$$\begin{aligned}
\tau^2(y,t;h_f) &= \frac{1}{V_0(t) - S_0(t)/V_0(t)} \sum_{i=1}^{n} \sum_{j=1}^{m_i} \left[W_{h_w}(y - y_i(t_{ij})) - \widehat{F}(y;t)\right]^2 K_{h_f}(t_{ij} - t), \\
V_0(t) &= \sum_{i=1}^{n} \sum_{j=1}^{m_i} K_{h_f}(t_{ij} - t), \\
S_0(t) &= \sum_{i=1}^{n} \sum_{j=1}^{m_i} K_{h_f}(t_{ij} - t)^2.
\end{aligned}$$

Then, h_f can be chosen by minimizing $\mathrm{RSC}(h_f)$.

2.2 Online Dynamic Process Monitoring

Now, we would like to construct an online monitoring procedure to sequentially monitor a new dynamic procedure (e.g., a new patient in the Framingham heart study discussed in Section 1) to see whether its longitudinal pattern is significantly different from the regular longitudinal pattern

that has been estimated by the method discussed in Subsection 2.1. If a significant difference is detected, then a signal will be given as soon as possible. The construction of such an online monitoring procedure is discussed below.

Assume that observations of the new dynamic process are obtained sequentially at times $\{t_1^*, t_2^*, \ldots\}$, and the corresponding observations are denoted as $\{y^*(t_1^*), y^*(t_2^*), \ldots\}$. In the above notations, the symbol "*" is used to denote that the observation times $\{t_1^*, t_2^*, \ldots\}$ could be different from those in the IC data, and the new dynamic process could be different from those in the IC data as well. However, it is assumed that if the new dynamic process is IC, then its time-varying process distribution should be the same as the process distribution of the regular longitudinal pattern, which is $F(q;t)$ discussed in Subsection 2.1. To monitor the new dynamic process, the DySS method proposed in Qiu and Xiang (2014) first standardized the observations of the new process by computing

$$\widehat{\epsilon}(t_j^*) = \{y^*(t_j^*) - \widehat{\mu}(t_j^*)\}/\widehat{\sigma}(t_j^*),$$

where $\widehat{\mu}(t)$ and $\widehat{\sigma}(t)$ were the estimates of the IC process mean function $\mu(t)$ and the IC process standard deviation $\sigma(t)$. Then, a cumulative sum (CUSUM) control chart was applied to the standardized observations. As discussed in Section 1, this existing DySS method described the regular longitudinal pattern of an IC dynamic process by $\mu(t)$ and $\sigma(t)$, which was appropriate only in cases when the IC dynamic process was a Gaussian process. In practice, however, the Gaussian process assumption would be rarely valid. Thus, the efficiency of this DySS method can be improved.

In our proposed new method, the regular longitudinal pattern is described by the IC time-varying process distribution $F(q;t)$. We would like to standardize the observations $\{y^*(t_1^*), y^*(t_2^*), \ldots\}$ of the new dynamic process by using the entire distribution function $F(q;t)$, instead of just its mean $\mu(t)$ and standard deviation $\sigma(t)$. To this end, after $F(q;t)$ is estimated by $\widehat{F}(q;t)$ (cf., (1)), we consider the following transformation (cf., Hawkins 1969):

$$z_j^* = \Phi^{-1}\left[\widehat{F}\left(y^*(t_j^*); t_j^*\right)\right], \tag{2}$$

where $\Phi^{-1}(\cdot)$ is the inverse function of the standard normal cdf. If the new dynamic process $y^*(t)$ is IC, then it is obvious that the distribution of $F\left(y^*(t_j^*); t_j^*\right)$ is Uniform(0,1) and the distribution of z_j^* is close to $N(0,1)$. Thus, when the observations $\{y^*(t_j^*), y^*(t_2^*), \ldots\}$ are independent of each other at different time points, it is natural to apply the following conventional CUSUM chart to

the transformed observations $\{z_j^*, j \geq 1\}$:

$$\begin{cases} \widetilde{C}_0^+ = 0, \\ \widetilde{C}_j^+ = \max\left(0, \widetilde{C}_{j-1}^+ + z_j^* - \widetilde{k}\right), \quad \text{for } j \geq 1, \end{cases} \tag{3}$$

where $\widetilde{k} > 0$ is an allowance constant. In the CUSUM chart (3), large values of z_j^* after a specific time point indicate an upward mean shift and will result in large values of the charting statistic $\widetilde{C}_j^+$. A signal for an upward distributional shift is then triggered at the time t_j^* if $\widetilde{C}_j^+ > \widetilde{\rho}$, where $\widetilde{\rho} > 0$ is a properly chosen control limit. Because upward mean shifts are our main concern in applications like the monitoring of cardiovascular disease risk factors (e.g., blood pressure readings) that was discussed in Section 1, the chart (3) is constructed for detecting upward mean shifts in $\{y^*(t_j^*), j \geq 1\}$. If our interest is in detecting a downward or arbitrary mean shift in a specific application, then the corresponding charts can be constructed in a similar way. See Chapter 4 in Qiu (2014) for a detailed discussion.

In practice, process observations at different time points are usually serially correlated. It has been well discussed in the literature that such data correlation should be taken into account in the design of the control chart and the chart would be unreliable to use otherwise (cf., Apley and Lee 2003, Apley and Shi 1999, Qiu et al. 2019). To handle the issue of data correlation, we try to decorrelate the transformed data (cf., (2)) and then apply the control chart to the decorrelated data, as discussed in Li and Qiu (2016). To this end, the serial data correlation structure should be estimated first from the IC dataset. Let

$$z_{ij} = \Phi^{-1}\big(\widehat{F}(y_i(t_{ij}), t_{ij})\big), \text{ for } j = 1, 2, \ldots, m_i, i = 1, 2, \ldots, n$$

be the transformed observations in the IC dataset, and $Q(s,t)$ be the covariance function of $\Phi^{-1}(\widehat{F}(y(t);t))$, for any $s, t \in [0,T]$. Then, $Q(s,t)$ can be estimated by the following local kernel estimate (cf., Qiu and Xiang 2015):

$$\widehat{Q}(s,t) = \frac{\sum_{i=1}^n \sum_{j_1,j_2=1,\ldots,m_i, j_1 \neq j_2} z_{ij_1} z_{ij_2} K_{h_\sigma}(t_{ij_1} - s) K_{h_\sigma}(t_{ij_2} - t)}{\sum_{i=1}^n \sum_{j_1,j_2=1,\ldots,m_i, j_1 \neq j_2} K_{h_\sigma}(t_{ij_1} - s) K_{h_\sigma}(t_{ij_2} - t)}, \quad \text{for } s \neq t,$$

and define $\widehat{Q}(s,t) = 1$ when $s = t$ since the transformed data are approximately standard normally distributed. The bandwidth parameter h_σ in the above expression can be selected by the cross-validation procedure, as discussed in Qiu and Xiang (2015).

After $Q(s,t)$ is estimated from the IC dataset, we can decorrelate the transformed data $\{z_j^*, j \geq 1\}$ of the new dynamic process under sequential monitoring. The specific data decor-

relation procedure used here was proposed by You and Qiu (2019), which is a more computationally efficient version of the one discussed in Li and Qiu (2016). This procedure starts by defining $U_1 = [\widehat{Q}(t_1^*, t_1^*)]^{-1/2}$. Then, the first standardized and decorrelated observation is defined to be

$$e_1^* = U_1 z_1^*.$$

For $j \geq 2$, the standardized and decorrelated version of z_j^* is defined by

$$e_j^* = \Big[z_j^* - \mathbf{v}_j'(e_1^*, e_2^*, \ldots, e_{j-1}^*)' \Big] \Big/ d_j,$$

where

$$\begin{aligned}
\mathbf{v}_j &= \mathbf{U}_{j-1}\Big(\widehat{Q}(t_1^*, t_j^*), \widehat{Q}(t_2^*, t_j^*), \ldots, \widehat{Q}(t_{j-1}^*, t_j^*)\Big)', \\
d_j &= \big[\widehat{Q}(t_j^*, t_j^*) - \mathbf{v}_j'\mathbf{v}_j\big]^{1/2}, \\
\mathbf{U}_j &= \begin{pmatrix} \mathbf{U}_{j-1} & \mathbf{0} \\ -\mathbf{v}_j'\mathbf{U}_{j-1}/d_j & 1/d_j \end{pmatrix}.
\end{aligned}$$

In the above expressions, d_j is a scalar, $\mathbf{v}_j$ is a $(j-1)$-dimensional vector, and $\mathbf{U}_j$ is a $j \times j$ matrix. To see how this decorrelation algorithm works, let $\mathbf{e}_j^* = (e_1^*, \ldots, e_j^*)'$ and $\mathbf{z}_j^* = (z_1^*, \ldots, z_j^*)'$. By the above definitions of e_j^* and $\mathbf{U}_j$, it can be seen that

$$\mathbf{e}_j^* = \mathbf{U}_j \mathbf{z}_j^*,$$

which means that each e_j^* is some linear combination of $z_1^*, \ldots, z_j^*$. By inversion matrix identity, we can show that

$$\begin{aligned}
\big[\mathbf{U}_j'\mathbf{U}_j\big]^{-1} &= \begin{pmatrix} \mathbf{U}_{j-1}'\mathbf{U}_{j-1} + \mathbf{U}_{j-1}'\mathbf{v}_j\mathbf{v}_j'\mathbf{U}_{j-1}/d_j^2 & -\mathbf{U}_{j-1}'\mathbf{v}_j/d_j^2 \\ -\mathbf{v}_j'\mathbf{U}_{j-1}/d_j^2 & 1/d_j^2 \end{pmatrix}^{-1} \\
&= \begin{pmatrix} \big[\mathbf{U}_{j-1}'\mathbf{U}_{j-1}\big]^{-1} & \mathbf{U}_{j-1}^{-1}\mathbf{v}_j \\ \mathbf{v}_j'\big[\mathbf{U}_{j-1}^{-1}\big]' & d_j^2 + \mathbf{v}_j'\mathbf{v}_j \end{pmatrix} \\
&= \begin{pmatrix} \big[\mathbf{U}_{j-1}'\mathbf{U}_{j-1}\big]^{-1} & \begin{pmatrix} \widehat{Q}(t_1^*, t_j^*) \\ \vdots \\ \widehat{Q}(t_{j-1}^*, t_j^*) \end{pmatrix} \\ \Big(\widehat{Q}(t_j^*, t_1^*), \cdots, \widehat{Q}(t_j^*, t_{j-1}^*)\Big) & \widehat{Q}(t_j^*, t_j^*) \end{pmatrix}.
\end{aligned}$$

Thus, by induction, we have $\left[\mathbf{U}_j'\mathbf{U}_j\right]^{-1} = \left\{\widehat{Q}(t_{k_1}^*, t_{k_2}^*)\right\}_{1\le,k_1,k_2\le j}$. Consequently, the variance of $\mathbf{e}_j^*$ is

$$\mathrm{Var}(\mathbf{e}_j^*) = \mathbf{U}_j\,\mathrm{Var}(\mathbf{z}_j^*)\mathbf{U}_j',$$

which is an identity matrix if $\widehat{Q}(s,t) = Q(s,t)$. Therefore, after the linear transformation $\mathbf{e}_j^* = \mathbf{U}_j\mathbf{z}_j^*$, $e_1^*, \ldots, e_j^*$ will be asymptotically uncorrelated and each of them will have the asymptotic mean of 0 and asymptotic variance of 1. Since the distribution of z_j^* is approximately $N(0,1)$, for each j, the distribution of e_j^* should be close to $N(0,1)$ as well since e_j^* is a linear combination of $z_1^*, z_2^*, \ldots, z_j^*$. After obtaining the standardized and decorrelated values $e_1^*, e_2^*, \ldots$, the following CUSUM chart can be applied to them for detecting upward distributional shifts in the original dynamic process:

$$\begin{cases} C_0^+ = 0, \\ C_j^+ = \max\left(0, C_{j-1}^+ + e_j^* - k\right), \quad \text{for } j \ge 1, \end{cases} \tag{4}$$

where $k > 0$ is an allowance constant. The chart gives a signal for an upward shift at the time t_j^* if $C_j^+ > \rho$, where $\rho > 0$ is a properly chosen control limit. This is the control chart that we propose in the paper for solving the DS problem, and is denoted as DySS-new hereafter.

To evaluate the performance of DySS-new in cases when observation times could be unequally spaced, we can use the IC average time to signal (ATS), denoted as ATS_0 and defined as the average time from the beginning of process monitoring to the signal time of the chart, and the OC ATS, denoted as ATS_1 and defined as the average time from the occurrence of a shift to the signal time. Usually, ATS_0 is fixed in advance, along with the allowance constant k. The control limit ρ is then computed (cf., the related discussion below) to achieve the given value of ATS_0. The chart performs better if its ATS_1 value is smaller for detecting a given shift.

From the above description about the proposed method DySS-new, it can be seen that it first transforms and decorrelates observations of a dynamic process with an arbitrary time-varying IC distribution to a sequence of standardized and uncorrelated observations $\{e_j^*, j \ge 1\}$ and then applies the conventional CUSUM chart to $\{e_j^*, j \ge 1\}$. The transformation and data decorrelation depend on the estimated functions $\widehat{F}(q;t)$ and $\widehat{Q}(s,t)$ obtained from the IC data. Under some regularity conditions, these estimated functions would converge to the true functions $F(q;t)$ and $Q(s,t)$ when the IC data size $M = \sum_{i=1}^n m_i$ increases. Thus, the IC distribution of $\{e_j^*, j \ge 1\}$ would be asymptotically $N(0,1)$ (Note: that IC distribution would be $N(0,1)$ if $F(q;t)$ and $Q(s,t)$ can be estimated perfectly well from the IC data). By this property, the control limit ρ of the

chart (4) can be determined by the Monte Carlo simulation, as described below. To accommodate unequally spaced observation times, Qiu and Xiang (2014) first suggested the concept of basic time unit, to denote the largest time unit that all unequally spaced observation times are its integer multiples. For instance, if all possible observation times are multiples of 7 days and there could be two consecutive observation times just 7-day apart, then the basic time unit is a week. Let d denote the average number of observation times within 10 consecutive multiples of the basic time unit. Then, d is a measure of the sampling rate. For a given value of d, a given value of k, and a desired level of ATS_0, the Monte Carlo simulation for determining the control limit ρ is described below.

Step 1. Generate an IC dataset with n dynamic processes. For the ith process, its observation times are generated from 1 to $10*M$ consecutive multiples of the basic time unit, by a random sampling algorithm so that d observation times are randomly selected without replacement from every 10 consecutive multiples of the basic time unit. The corresponding standardized and decorrelated values of the process observations are generated from the $N(0,1)$ distribution. The generated IC dataset is denoted as $\{(e_{ij}^{\text{mc}}, t_{ij}^{\text{mc}}), j = 1, 2, \ldots, d*M, i = 1, 2, \ldots, n\}$.

Step 2. For a given control limit ρ, apply the control chart (4) to the IC data generated in Step 1, and the ATS value is recorded.

Step 3. If the calculated ATS in Step 2 is within ϵ of the desired level of ATS_0, then the current value of ρ is exported as the selected control limit and the entire algorithm is finished. If the calculated ATS is smaller than $\text{ATS}_0 - \epsilon$, then the current value of ρ is increased and then Step 2 is repeated. If the calculated ATS is larger than $\text{ATS}_0 + \epsilon$, then the current value of ρ is decreased and then Step 2 is repeated.

In cases when $n = 100,000$, $M = 100$, $\epsilon = 10^{-5}$, $d = 1, 2$ or 5, $k = 0.1$ or 0.2, and the given level of ATS_0 is 100, 150, 200, 250, 300 or 370, the values of ρ determined by the above algorithm are presented in Table 1. These values can be used in practice for cases with the listed values of d, k and ATS_0 in the table. In cases when the values of d, k and ATS_0 cannot be found in the table, the corresponding values of ρ can be computed easily using the above algorithm.

Table 1: Calculated values of ρ of the CUSUM chart (4) in cases when $n = 100,000$, $M = 100$, $\epsilon = 0.1$, $d = 1, 2$ or 5, $k = 0.1$ or 0.2, and the given level of ATS_0 is 100, 150, 200, 250, 300 or 370.

	$d=1$		$d=2$		$d=5$	
ATS_0	$k=0.1$	$k=0.2$	$k=0.1$	$k=0.2$	$k=0.1$	$k=0.2$
100	1.756	1.500	2.764	2.318	4.570	3.676
150	2.308	1.959	3.494	2.884	5.568	4.394
200	2.768	2.323	4.093	3.335	6.363	4.941
250	3.176	2.641	4.607	3.713	7.048	5.394
300	3.545	2.929	5.081	4.049	7.668	5.796
370	4.045	3.309	5.691	4.487	8.473	6.315

3 Simulation Study

In this section, we present some simulation studies to evaluate the numerical performance of the proposed method. In these examples, all observation times are in the time interval $[0, 1]$, the basic time unit is $\omega = 0.001$, and $M = 100$. Thus, all observation times are in the set $\mathbb{T} = \{\omega, 2\omega, \ldots, 1000\omega\}$. We consider 6 different cases for the IC longitudinal pattern. In cases (I)-(III), the IC dynamic processes are assumed to follow the model

$$y_i(t) = \mu(t) + \sigma(t)\epsilon_i(t), \tag{5}$$

where $\mu(t) = \cos(\pi t)$, $\sigma(t) = 1 + 0.2\sin(3\pi t)$, and $\epsilon_i(t)$ is a random error process. In these three cases, $\{\epsilon_i(t) : t \in \mathbb{T}\}$ are generated independently from the following three distributions: $N(0, 1)$ in case (I), standardized version with mean 0 and variance 1 of the χ^2_5 distribution in case (II), and standardized version with mean 0 and variance 1 of the $t_{2.5}$ distribution in case (III). These three cases represent three scenarios with a symmetric light-tailed error distribution, a skewed error distribution, and a symmetric heavy-tailed error distribution. In case (III), the degree of freedom of 2.5 is chosen since the variance of $t_{2.5}$ is well defined and $t_{2.5}$ has a heavy tail. In cases (IV)-(VI), the IC dynamic processes are assumed to follow the following nonparametric mixed-effects model

$$y_i(t) = \mu(t) + \xi_{i1}u_1(t) + \xi_{i2}u_2(t) + \xi_{i3}u_3(t) + 0.5\epsilon_i(t), \tag{6}$$

where $\mu(t) = -\sin(t)$, $u_1(t) = t(1-t)$, $u_2(t) = (1-t)/2$, $u_3(t) = \log(1+t)$, the random effects ξ_{i1}, ξ_{i2} and ξ_{i3} are independent and identically distributed with the common distribution of $N(0, 1)$,

and the random error terms $\{\epsilon_i(t) : t \in \mathbb{T}\}$ are generated in the same ways as those in cases (I)-(III), respectively.

In all cases considered in this section, the sampling rate d is set to be 2. The allowance constant k in the CUSUM chart (4) is chosen to be 0.1 or 0.2, and its control limit is chosen by the procedure described at the end of Section 2. Besides the proposed method DySS-new, we will also consider four other methods for comparison purposes, including the method by Qiu and Xiang (2014), the method by Li and Qiu (2016), the method that monitors z_j^* directly (which can be accomplished by replacing e_j^* by z_j^* in the chart (4)), and the method by You and Qiu (2019). In the method by Qiu and Xiang (2014), the conventional CUSUM chart is applied directly to the standardized observations $\{\widehat{\epsilon}(t_j^*) = [y^*(t_j^*) - \widehat{\mu}(t_j^*)]/\widehat{\sigma}(t_j^*)\}$, where $\widehat{\mu}(t)$ and $\widehat{\sigma}^2(t)$ are estimates of the IC process mean function $\mu(t)$ and the IC process variance function $\sigma^2(t)$. Its control limit is determined by simulations based on the assumptions that the standardized observations $\{\widehat{\epsilon}(t_j^*)\}$ are i.i.d. with the common distribution of $N(0,1)$ when the process is IC. This method is denoted as DySS-std hereafter. The method by Li and Qiu (2016) decorrelated the standardized observations $\{\widehat{\epsilon}(t_j^*)\}$ first, and then applied the conventional CUSUM chart to the decorrelated data. Its control limit is chosen by simulations as well based on the assumption that the decorrelated standardized observations are i.i.d. with the common IC distribution of $N(0,1)$. This method is denoted as DySS-dec hereafter. As discussed in Section 1, both of these two competing methods described the regular longitudinal pattern of an IC dynamic process by using the IC process mean function $\mu(t)$ and the IC process variance function $\sigma^2(t)$ only, which may not be good enough in cases when the IC process distribution is skewed or heavy-tailed, such as the cases (II), (III), (V) and (VI) discussed above. The alternative method that monitors the transformed observations z_j^* directly is denoted by DySS-dir. Its control limit is chosen in the same way as that for DySS-new. This method considered the IC process distribution through the transformation (2), but ignored possible correlation among process observations in its chart construction. Thus, it may not perform well in cases (IV)-(VI) when the process observations are correlated. The method by You and Qiu (2019) proposed to make use of the restarting mechanism of a CUSUM chart when decorrelating process observations. By the restarting mechanism, it only decorrelates a small portion of the previous process observations that are collected after the last time that the CUSUM chart is reset to 0. In the literature, the number of observation times after the last time the CUSUM chart is reset to 0 is called "sprint length" (Chatterjee and Qiu 2009). The method by You and Qiu (2019) is denoted

by DySS-spr. Its control limit is chosen by a bootstrap procedure from the IC data, as suggested in You and Qiu (2019). As a comparison, our proposed method DySS-new described the regular longitudinal pattern by using the entire cdf of the IC process distribution. It should be more robust to the shape of the IC process distribution, which will be confirmed below.

We first evaluate the IC performance of the five methods. In this simulation example, the IC sample size is set to be 100, 200 or 500, the nominal ATS_0 value is set to be 370, and the control limits of the charts are selected by using the Monte Carlo algorithm described in Section 2.2. For each method, its actual ATS_0 values are calculated as follows. First, an IC dataset is generated and the IC mean function, the IC variance function and the IC cdf are computed from the IC dataset. Second, the ATS_0 value of the method is computed by applying the related control chart to the simulated data of 2,000 IC dynamic processes. Finally, the previous two steps are repeated for 200 times, and the actual ATS_0 value is computed to be the sample mean of the 200 ATS_0 values obtained from the 200 replicated simulations. The standard error of the actual ATS_0 value can also be calculated from the 200 ATS_0 values, as their standard deviation divided by $\sqrt{200}$. The calculated actual ATS_0 values of the five methods in cases (I)-(VI) are presented in Table 2. In the table, those actual ATS_0 values which are within 10% of the nominal ATS_0 level of 370 are in bold. From the table, we can see that our proposed method DySS-new is indeed robust to different IC time-varying process distributions considered in this example, since its actual ATS_0 values are close to the nominal ATS_0 level of 370 in all cases considered. As a comparison, the method DySS-std has a reliable IC performance only in case (I) and in case (II) with $k = 0.2$. In all other cases, its actual ATS_0 values are substantially different from the nominal ATS_0 level. Besides the reason given in the previous paragraph that this method cannot accommodate skewed or heavy-tailed IC process distributions properly, it cannot accommodate serial data correlation in cases (IV)-(VI) either. The method DySS-dec improves DySS-std in cases (IV)-(VI) when there is serial data correlation, as expected, since the former decorrelates the standardizes observations $\{\widehat{\epsilon}(t_j^*)\}$ before process monitoring. But, its performance in cases when the IC process distribution is skewed or heavy-tailed is still unreliable. The method DySS-dir takes the IC process distribution into account whereas ignores the serial data correlation. As a consequence, it is robust to the distribution of data when serial data correlation does not exist in cases (I)-(III). However, in cases (IV-VI) when serial data correlation exists, it fails to achieve the desired IC performance. The method DySS-spr relies on the block bootstrap procedure for selection of control limit. The original IC samples will

be partitioned into two parts with one part for model estimation and the other part for selection of the control limit. Although this method can approximately attain the desired IC ATS in most cases considered here, its standard error of IC ATS is much larger than that of the proposed method. This suggests that the variability of IC ATS of DySS-spr is much higher than that of the proposed method.

Next, we evaluate the OC performance of the related methods. In the following example, the ATS_0 value is still fixed at 370, the IC sample size is fixed at $n = 500$, and the OC process observations are generated from the model

$$y^*(t) = \begin{cases} y(t), & \text{for } t \leq 0.05 \\ y(t) + \delta, & \text{for } t > 0.05, \end{cases} \tag{7}$$

where $y(t)$ follows the models (5) and (6), and $\delta \geq 0$ is an upward shift that occurs at time 0.05. The upward shift size δ changes from 0.0 to 1.0 with a step of 0.1. To make the comparison fair, the control limits of the related charts have been adjusted so that all methods have their actual ATS_0 values being 370. Then, in each case considered, the ATS_1 value of each method is calculated in the same way as that for calculating the actual ATS_0 value, except that process observations are generated from (7) here. The calculated ATS_1 values of the five charts are presented in Figure 1. From the figure, it can be seen that i) the OC performance of the five charts is almost identical in case (I), ii) DySS-new and DySS-dir are better than DySS-std, DySS-dec, and DySS-spr in cases (II) and (III), iii) the performance of DySS-new and DySS-dec are similar in cases (IV)-(VI) and both of them are much better than DySS-std, DySS-dist and DySS-spr. So, this example shows that the proposed method DySS-new would have the best OC performance in all cases considered, although its OC performance could be similar to that of DySS-dir in certain cases when process observations are independent, and similar to that of DySS-dec in certain cases when serial data correlation exists. By combining the results in this example and the results in Table 2, DySS-new can indeed provide a more reliable and effective solution to the DS applications, compared to the alternative methods DySS-std, DySS-dec, DySS-dir and DySS-spr.

Table 2: Calculated actual ATS_0 values in cases (I)-(VI), when $n = 100, 200, 500$, $k = 0.1, 0.2$, and the nominal ATS_0 value is 370. Numbers in bold denote those within 10% of the nominal ATS_0 value. Numbers in parentheses are the corresponding standard errors.

k	Case	n	DySS-std	DySS-dec	DySS-dir	DySS-spr	DySS-new
0.1	(I)	100	**362.8** (1.3)	**355.2** (1.4)	**373.2** (1.3)	**375.8** (3.1)	**362.3** (1.4)
		200	**363.0** (0.9)	**358.8** (1.0)	**371.1** (1.0)	**369.3** (2.0)	**366.8** (1.0)
		500	**363.3** (0.8)	**361.9** (0.8)	**371.0** (0.8)	**368.4** (1.4)	**369.4** (0.8)
	(II)	100	**343.5** (1.3)	**337.4** (1.2)	**362.2** (1.3)	**369.7** (2.6)	**353.3** (1.2)
		200	**344.3** (1.0)	**341.7** (1.1)	**365.8** (1.0)	**372.4** (2.0)	**362.0** (1.1)
		500	**344.9** (0.7)	**343.5** (0.7)	**368.0** (0.7)	**370.4** (1.4)	**366.1** (0.8)
	(III)	100	516.0 (3.5)	502.5 (3.5)	**369.7** (1.3)	**379.2** (3.1)	**362.8** (1.4)
		200	536.2 (3.2)	528.7 (3.1)	**374.8** (1.0)	**371.2** (2.0)	**371.1** (1.1)
		500	541.3 (2.6)	538.0 (2.7)	**376.0** (0.6)	**371.3** (1.4)	**374.1** (0.7)
	(IV)	100	495.6 (2.6)	**359.9** (1.4)	500.9 (2.6)	**367.8** (4.1)	**374.6** (1.5)
		200	497.2 (1.8)	**365.8** (1.1)	500.9 (1.3)	**370.4** (2.8)	**377.0** (1.1)
		500	498.0 (1.4)	**369.2** (0.8)	500.5 (1.0)	**369.6** (2.0)	**376.8** (0.8)
	(V)	100	494.9 (2.7)	**340.7** (1.3)	480.8 (2.7)	**366.2** (3.9)	**362.1** (1.2)
		200	493.6 (1.9)	**344.8** (0.9)	481.5 (1.9)	**370.1** (2.5)	**362.2** (0.8)
		500	492.1 (1.3)	**346.0** (0.7)	481.4 (1.2)	**369.3** (1.9)	**360.3** (0.6)
	(VI)	100	494.9 (2.7)	445.2 (2.8)	489.5 (2.6)	**373.1** (3.8)	**387.3** (1.3)
		200	494.1 (1.7)	459.8 (2.5)	490.9 (1.8)	**366.6** (2.7)	**388.1** (1.1)
		500	498.2 (1.3)	477.8 (2.4)	495.4 (1.3)	**372.8** (1.7)	**386.2** (1.0)
0.2	(I)	100	**363.8** (1.2)	**355.8** (1.3)	**375.6** (1.3)	**375.1** (3.1)	**363.2** (1.3)
		200	**364.1** (0.9)	**359.5** (1.0)	**372.7** (1.0)	**369.3** (2.1)	**368.2** (1.0)
		500	**364.2** (0.8)	**362.5** (0.8)	**372.0** (0.8)	**369.2** (1.4)	**370.3** (0.8)
	(II)	100	310.4 (1.2)	305.6 (1.1)	**363.9** (1.3)	**370.5** (2.8)	**354.3** (1.2)
		200	311.2 (1.0)	309.2 (1.0)	**368.0** (1.0)	**371.3** (2.2)	**363.6** (1.0)
		500	311.6 (0.7)	310.6 (0.7)	**370.0** (0.7)	**370.3** (1.5)	**368.0** (0.8)
	(III)	100	531.2 (3.5)	518.8 (3.6)	**373.1** (1.3)	**378.7** (3.1)	**365.5** (1.4)
		200	553.3 (3.2)	547.0 (3.1)	**377.7** (1.0)	**370.9** (2.1)	**374.0** (1.1)
		500	558.7 (2.6)	555.6 (2.6)	**378.2** (0.7)	**372.3** (1.4)	**376.4** (0.7)
	(IV)	100	513.4 (2.6)	**359.5** (1.3)	519.6 (2.6)	**368.2** (4.0)	**379.8** (1.4)
		200	515.3 (1.9)	**365.3** (1.0)	519.8 (1.3)	**371.3** (2.9)	**381.0** (1.1)
		500	516.3 (1.4)	**369.3** (0.8)	519.3 (1.0)	**369.7** (2.0)	**379.9** (0.8)
	(V)	100	501.8 (2.7)	310.5 (1.2)	495.2 (2.8)	**367.3** (3.9)	**349.0** (1.1)
		200	500.9 (1.9)	314.5 (0.9)	496.4 (1.9)	**369.4** (2.5)	**348.3** (0.8)
		500	499.2 (1.3)	315.5 (0.6)	496.3 (1.3)	**368.4** (1.9)	**344.7** (0.6)
	(VI)	100	506.3 (2.7)	462.9 (3.2)	506.4 (2.6)	**372.0** (3.6)	**385.2** (1.3)
		200	506.1 (1.8)	479.8 (2.9)	508.6 (1.8)	**367.1** (2.7)	**384.4** (1.0)
		500	511.1 (1.4)	500.6 (2.7)	513.0 (1.3)	**371.6** (1.7)	**381.8** (1.1)

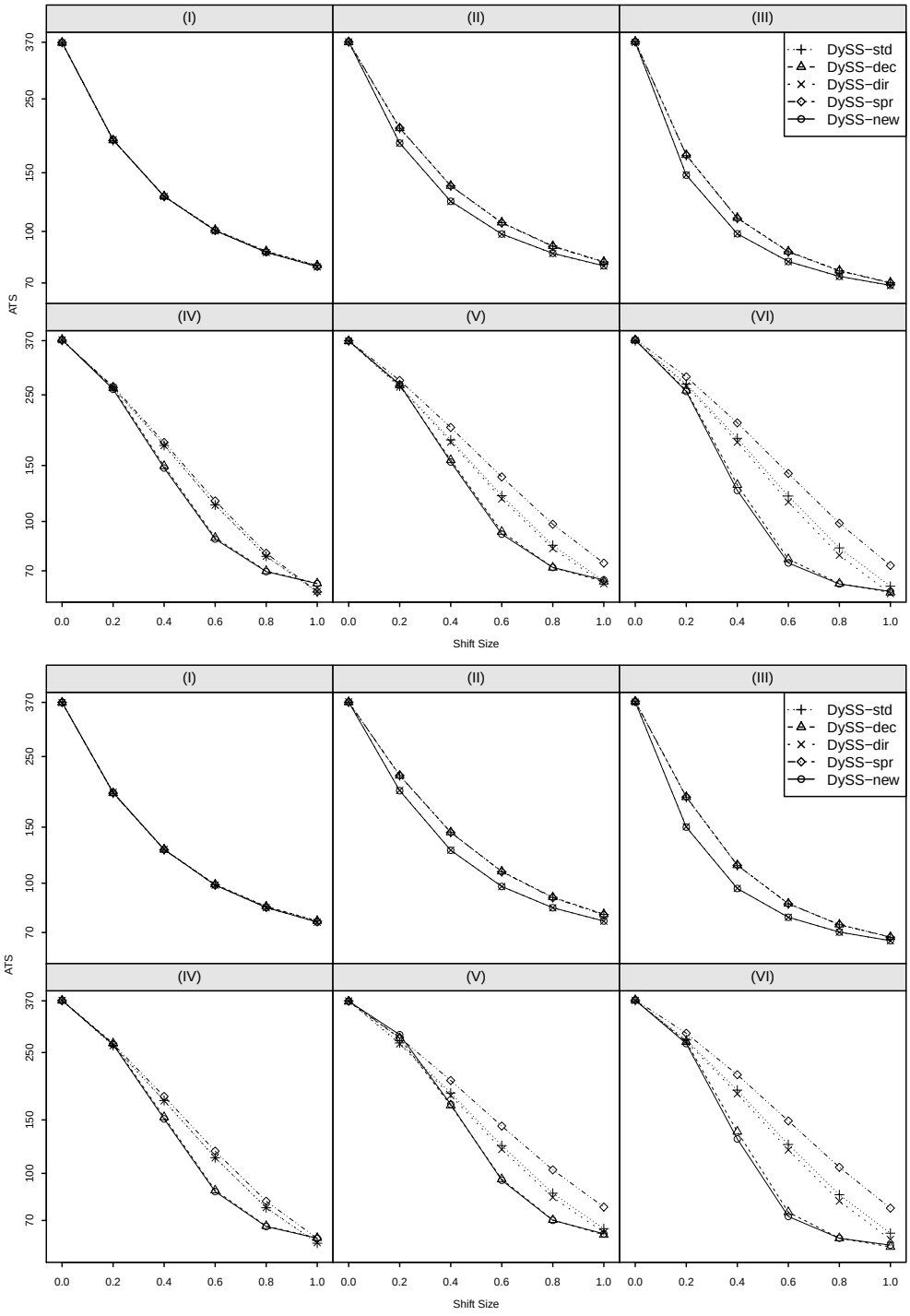

Figure 1: Calculated ATS_1 values of the five DySS methods in cases (I)-(VI) when the IC sample size is $n = 500$, the ATS_0 value is 370, and the allowance constant k is fixed at 0.1 (two top rows) and 0.2 (two bottom rows).

4 A Real-Data Application

In this section, we present an application of the proposed DySS method. The data considered here were obtained from the well-known Framingham heart study in which scientists were mainly concerned about the risk factors of cardiovascular diseases (cf., Cupples et al. 2007). The data contain systolic blood pressure readings of 1,055 patients, among which 27 patients had strokes during the study and the other 1,028 did not. In the study, each patient was followed for 7 times at different ages. The readings of the systolic blood pressure of all patients are displayed in the left panel of Figure 2, in which the dark dashed lines denote the longitudinal observations of the stroke patients and the gray solid lines denote the longitudinal observations of the non-stroke patients. In this example, the observed data of the 1,028 non-stroke patients are used as the IC data, the data of the 27 stroke patients are used for testing the proposed method. The histogram of the observed data of the 1,028 non-stroke patients is shown in the right panel of Figure 2, from which it can be seen that the IC distribution of the systolic blood pressure is moderately skewed to the right. As a matter of fact, the sample skewness can be calculated to be 0.721 with the 95% CI being (0.665,0.778), which confirms the significant positive skewness. The p-value of the Shapiro-Wilk normality test is $< 10^{-5}$, indicating that the distribution is significantly different from normal. We also examined the serial data correlation among observations. After removing the mean from the observed data by using the estimated mean function from the IC data, the estimated correlation coefficient between two adjacent observations is 0.582 with the 95% CI being (0.566,0.599). The corresponding test for zero correlation between two adjacent observations gives a p-value that is $< 2.2 \times 10^{-16}$, which provides a significant evidence for serial correlation between two adjacent observations.

To apply our proposed method DySS-new to this data, we first need to compute the estimated cdf from the IC data (cf., (1)), and then transform (cf., (2)) and decorrelate the test data, as discussed in Subsection 2.2. The control limit of the chart (4) should also be determined using the procedure described at the end of Section 2, in which observation times of a simulated dynamic process are obtained by i) randomly selecting a patient from the 1,028 non-stroke patients in the IC data with replacement, and ii) using the observation times of the selected patient in step i). In the chart, the allowance constant k is chosen to be 0.1 and the ATS_0 level is set to be 30 years. The chosen value for k has been used in the simulation examples in Section 3, and the chosen ATS_0

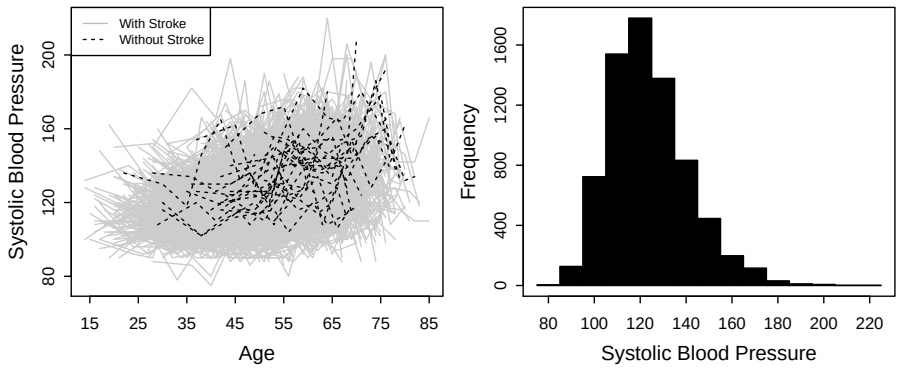

Figure 2: The systolic blood pressure readings (left panel) of 1,028 non-stroke patients (gray solid lines) and 27 stroke patients (dark dashed lines), and the histogram (right panel) of the systolic blood pressure readings of the 1,028 non-stroke patients.

level of 30 years should be reasonable in the context of this example since it should be acceptable for non-stroke patients to have the expected time to a false signal being as long as 30 years. The chart of DySS-new for monitoring the 27 stroke patients are shown in the bottom panel of Figure 3, from which it can be seen that 22 stroke patients receive signals from the chart. As a comparison, the charts of DySS-std, DySS-dec, DySS-dir and DySS-spr for monitoring the same group of stroke patients are shown in the top four panels of Figure 3. In these charts, the same values of k and ATS_0 are used as those in DySS-new. From the figure, it can be seen that the number of patients receiving signals from the charts DySS-std, DySS-dec, DySS-dir and DySS-spr are 19, 21, 19 and 21, respectively. Also, the ATS_1 value of the proposed method DySS-new is 19.1 years, while the ATS_1 values of DySS-std, DySS-dec, DySS-dir and DySS-spr are 21.1 years, 20.5 years, 21.2 years, and 25.2 years, respectively. Thus, in this example, DySS-new gives more signals to stroke patients with a shorter ATS_1 value, compared to the four competing methods.

5 Discussion and Concluding Remarks

In this paper, a new and effective DySS method has been proposed, which is based on estimation of the entire IC process distribution of a dynamic process following the regular longitudinal pattern. Numerical studies have shown that it is indeed more effective than some representative existing DySS methods in various cases considered. However, there are still some issues about the new method that need to be addressed in our future research. First, the proposed method DySS-new

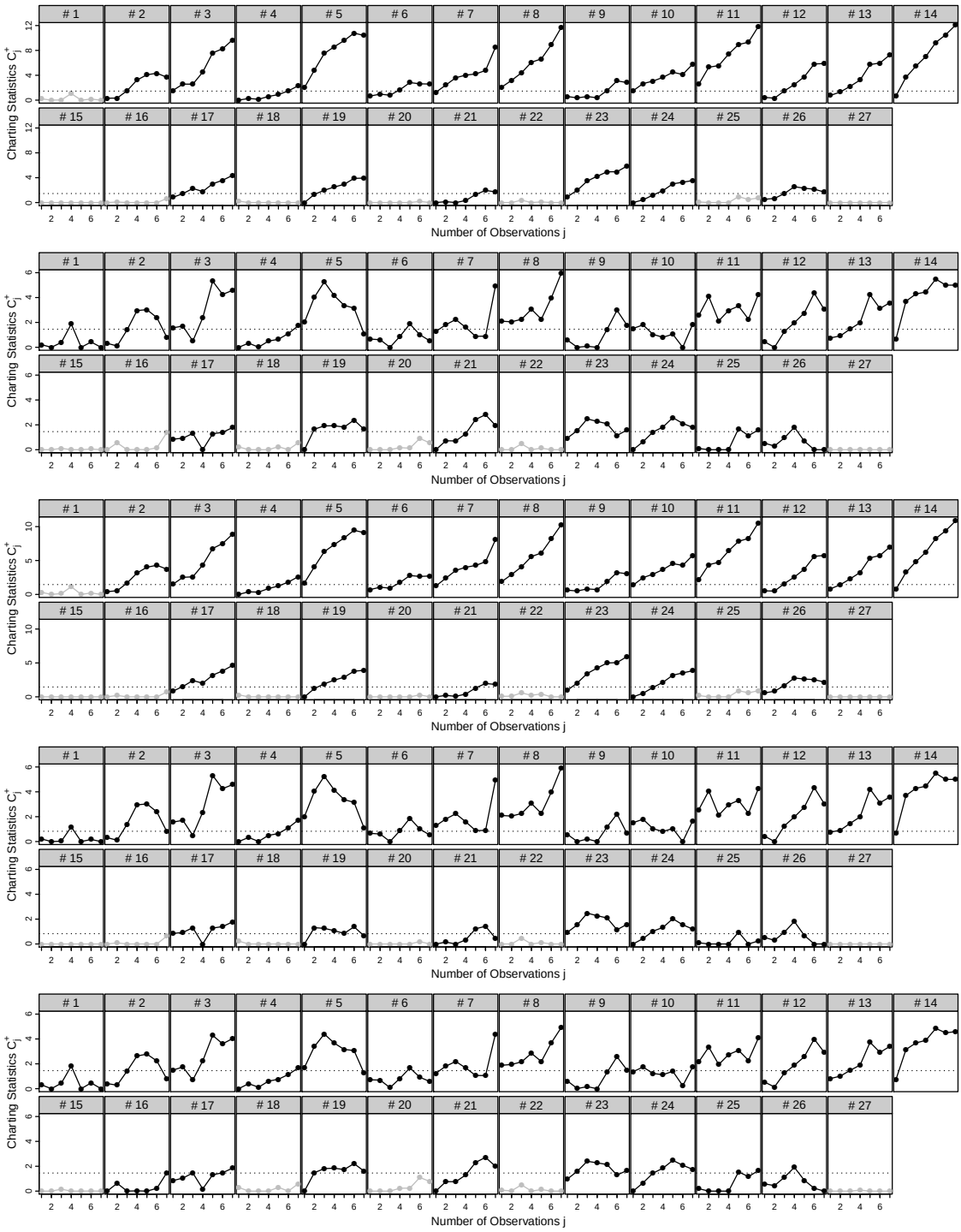

Figure 3: Charting statistics of five different methods for monitoring 27 stroke patients (from top to bottom: DySS-std, DySS-dec, DySS-dir, DySS-spr and DySS-new). Control charts in dark denote cases with signals, and those in gray denote cases without signals.

requires a relatively large IC dataset to estimate the cdf of the IC process distribution. In many applications such as the one discussed in Section 4, this may not be a problem. But, in some applications, a relatively large IC dataset may not be available. In such cases, self-starting control charts might be helpful (cf., Hawkins 1987), which will be studied carefully in our future research. Second, although the proposed method is more robust to the IC process distribution, compared to some existing methods, there is room for improvement in computing the control limit of the chart (4) using the Monte Carlo searching algorithm described at the end of Section 2. The reason is that transformed and standardized process observations are assumed to be independent in the Monte Carlo searching algorithm, but the transformed and standardized process observations are only guaranteed to be asymptotically uncorrelated. Some theoretical study is needed to figure out conditions under which the independence assumption is (asymptotically) valid, although simulation results in Table 2 have shown that results based on the independence assumption are reasonably good in all cases considered there. To address this issue, some research in multivariate copula modelling (cf., Smith et al. 2010) and in monitoring of serially correlated data (cf., Qiu et al. 2019) might be helpful, which will be investigated in our future research. Third, in many applications, one may wish to use available covariate information in process monitoring. In the literature, several modeling approaches have been proposed to accommodate covariates. For example, Wu and Tian (2013) used a time-varying transformation model to describe the conditional distribution of $y(t)$ given some covariates. However, their method requires that the number of observations obtained at each observation time point is relatively large and the linkage function that connects the longitudinal outcome and covariates is known and pre-specified. These requirements are difficult to meet in many DS problems. This topic will be investigated in our future research. Last but not the least, in some DS problems, the observation time scale could be uninformative, and the origins of different dynamic processes can be all different. In such cases, proper alignment of dynamic processes becomes an important issue. There have been several methods for aligning time series data with equally spaced observation times (e.g., Colosimo and Pacella 2007). Because the observation times could be unequally spaced in some DS problems, temporal alignment of different dynamic processes could be trickier than the alignment of equally spaced time series data. The issue to align different dynamic processes when the observation time scale is uninformative will be left for our future research.

Acknowledgments: We thank the editor and two referees for many constructive comments

and suggestions, which improved the quality of the paper greatly. This research is supported in part by the NSF grant DMS-1914639.

References

Apley, D.W., and Lee, H.C. (2003), "Design of exponentially weighted moving average control charts for autocorrelated processes with model uncertainty," *Technometrics*, **45**, 187–198.

Apley, D.W., and Shi, J. (1999), "The GLRT for statistical process control of autocorrelated processes," *IIE Transactions*, **31**, 1123–1134.

Chatterjee, S., and Qiu, P. (2009), "Distribution-free cumulative sum control charts using bootstrap-based control limits," *Annals of Applied Statistics*, **3**, 349–369.

Colosimo, B. M. and Pacella, M. (2007), "On the use of principal component analysis to identify systematic patterns in roundness profiles", *Quality and Reliability Engineering International*, **23**, 707–725

Cupples, L.A. et al. (2007), "The Framingham Heart Study 100K SNP genome-wide association study resource: overview of 17 phenotype working group reports," *BMC Medical Genetics*, **8**, (Suppl 1): S1.

Epanechnikov, V. A. (1969), "Non-parametric estimation of a multivariate probability density", *Theory of Probability & Its Applications*, **14**, 153–158.

Fan, J., and Gijbels, I. (1995), "Data-driven bandwidth selection in local polynomial fitting: variable bandwidth and spatial adaptation", *Journal of the Royal Statistical Society: Series B (Methodological)*, **57**, 371–394.

Fan, J., Yao, Q., and Tong, H. (1996), "Estimation of conditional densities and sensitivity measures in nonlinear dynamical systems", *Biometrika*, **83**, 189–206.

Hawkins, D.M. (1969), "On the distribution and power of a test for a single outlier," *South African Statistical Journal*, **3**, 9–15.

Hawkins, D.M. (1987), "Self-starting cusums for location and scales," *The Statistician,* **36**, 299–315.

Hawkins, D.M., and Olwell, D.H. (1998), *Cumulative Sum Charts and Charting for Quality Improvement*, New York: Springer-Verlag.

Kang, L., and Albin, S.L. (2000), "On-line monitoring when the process yields a linear profile," *Journal of Quality Technology*, **32**, 418–426.

Li, J. and Qiu, P. (2016), "Nonparametric dynamic screening system for monitoring correlated longitudinal data", *IIE Transactions*, **48**, 772–786.

Li, J. and Qiu, P. (2017), "Construction of an efficient multivariate dynamic screening system", *Quality and Reliability Engineering International*, **33**, 1969–1981.

Li, W., Dou, W., Pu, X., and Xiang, D. (2018), "Monitoring individuals with irregular semiparametric longitudinal behaviour," *Quality Technology & Quantitative Management*, **15**, 37–52.

Montgomery, D.C. (2012), *Introduction to Statistical Quality Control*, New York: John Wiley & Sons.

Qiu, P. (2014), *Introduction to Statistical Process Control*, Boca Raton, FL: Chapman Hall/CRC.

Qiu, P., Li, W., and Li, J. (2020), "A new process control chart for monitoring short-range serially correlated data", *Technometrics*, **62**, 71–83.

Qiu, P. and Xiang, D. (2014), "Univariate dynamic screening system: an approach for identifying individuals with irregular longitudinal behavior", *Technometrics*, **56**, 248–260.

Qiu, P. and Xiang, D. (2015), "Surveillance of cardiovascular diseases using a multivariate dynamic screening system", *Statistics in Medicine*, **34**, 2204–2221.

Qiu, P., Zi, X., and Zou, C. (2018), "Nonparametric dynamic curve monitoring", *Technometrics*, **60**, 386–397.

Qiu, P., Zou, C., and Wang, Z. (2010), "Nonparametric profile monitoring by mixed effects modeling (with discussions)," *Technometrics*, **52**, 265–277.

Silverman, B.W. (2018), *Density Estimation For Statistics and Data Analysis*, Chapman & Hall.

Smith, M., Min, A., Almeida, C., and Czado, C. (2010), "Modeling longitudinal data using a pair-copula decomposition of serial dependence", *Journal of the American Statistical Association*, **105**, 1467–1479.

Wu, C. O. and Tian, X. (2013), "Nonparametric estimation of conditional distributions and rank-tracking probabilities with time-varying transformation models in longitudinal studies", *Journal of the American Statistical Association*, **108**, 971–982.

You, L. and Qiu, P. (2019), "Fast computing for dynamic screening systems when analyzing correlated data", *Journal of Statistical Computation and Simulation*, **89**, 379–394.

Yu, K. and Jones, M. (1998), "Local linear quantile regression", *Journal of the American Statistical Association*, **93**, 228–237.